

Identifying Microlensing by Binaries

Rosanne Di Stefano and Rosalba Perna

Harvard-Smithsonian Center for Astrophysics, Cambridge, MA 02138

Received _____; accepted _____

ABSTRACT

The microlensing monitoring programs have studied large numbers of standard light curves which seem to be due to lensing by a dark point mass. Theory predicts that many microlensing events should display significant deviations from the standard form. Lens binarity in particular is expected to be common. So far, however, only a handful of light curves exhibit evidence that the lens is a binary; all of these display dramatic deviations from the standard light curve, exhibiting pronounced multiple peaks and/or caustic crossings.

Binary-lens events in which the light curve is less dramatically perturbed should also exist in the data set. Why, then, have we not detected them? The answer may lie in the fact that the perturbations, though often significant, tend to be less distinctive than those associated with caustic crossings. It is therefore possible that some of these more gently perturbed events have been misclassified, and that others have simply been missed. Reliable estimates of the overall detection efficiency, hence derivation of the fraction of the Halo mass that may be in MACHOs, rely on resolving this issue. Microlensing can also be used to determine the form of the initial mass function (IMF) beyond the solar neighborhood; accurate determination of the IMF also relies on the ability to correctly identify binary light curves.

We present a method to determine whether a light curve is due to lensing by a binary. The method works for both gently and dramatically perturbed binary lens light curves. Our method identifies all degenerate solutions—i.e., all possible lensing events that might have given rise to the observed light curve. It also enables us to eliminate from consideration large ranges of possible false positive identifications associated with light curves that might mimic microlensing by a binary. This method, or a generalization of it, can also be applied to the analysis of light curves that deviate from the standard point-mass lens form because of astronomical effects other than lens binarity.

Subject headings: dark matter – gravitational lensing – stars:
low-mass, brown dwarfs

1. Introduction

Given a light curve, how can we determine whether it is associated with a microlensing event? It is relatively easy to answer this question if a single dark mass lenses a point source in an otherwise blank field (see, e.g., Paczyński 1986). This, however, is not the case expected to be most commonly encountered in the microlensing observations. Source and lens binarity (Griest & Hu 1992; Mao & Paczyński 1991; Mao & Di Stefano 1995; Udalski *et al.* 1994; Di Stefano & Mao 1996; Di Stefano 1996), blending (Udalski *et al.* 1994; Di Stefano & Esin 1995; Kamionkowski 1995; Buchalter, Kamionkowski, & Rich 1996), and finite source size effects (Witt & Mao 1994; Witt 1995) are expected to play a role in a large fraction of microlensing events. The associated light curves will not be of the standard form. Some will be relatively mild perturbations of the standard form. Others will be dramatically different. The presence of these non-standard light curves in the data sets presents a challenge to the analysis of the ensemble of events. Without systematic methods to reliably recognize that they do correspond to microlensing events, the detection efficiency is diminished and its numerical value uncertain. If the observing teams are to achieve their goal of quantifying the size and characteristics of compact dark objects in the Local Group, it is therefore crucial that they develop the ability to discover and study a wide range of non-standard light curves in addition to those due to lensing by a point mass.

In this paper we focus on the problem of identifying light curves due to lensing by a binary. A first attempt to solve this problem was made by Mao & Di Stefano (1995), who found that the timing of maxima and minima could be used as a first step toward identifying all possible physical events that might have given rise to a multiply-peaked light curve, particularly if some of the peaks are due to caustic crossings. Their method was used to study the first detected binary lens (Udalski *et al.* 1994; Alcock *et al.* 1996). Today, the observing teams each have the capability of analyzing strongly perturbed binary-lens light curves. Until now, however, the more gently perturbed light curves which should also be present in the data set have neither been classified nor detected.

1.1. Expected Numbers

Figure 1 shows 15 light curves. These have been randomly generated, with all of the physical variables (§2.1) chosen from uniform probability distributions. (See the figure caption.) The light curves with sharply rising and falling wall-like structures represent events in which the track of the source has crossed through caustic curves. It is interesting

that OGLE 7, the first discovered binary lens microlensing event (Udalski *et al.* 1994; Alcock *et al.* 1996) exhibits the double wall structure found in 3 of the light curves shown. It is also interesting that approximately 8 of these 15 randomly chosen curves are relatively gentle perturbations of the standard point mass lens light curve, of a sort that has not yet been reliably identified in the data set. The fractions expected in the data sets of single-peak and multiple-peak light curves, of light curves exhibiting caustic crossings, and of light curves exhibiting the more gentle perturbations cannot be inferred from this graph. The number of light curves shown is too small, and the underlying distribution of values of mass ratios and orbital separations among the population of binary lenses is not likely to be uniform. Nevertheless, this simple exercise provides insight consistent with a more detailed consideration of the statistics of binary lensing (Di Stefano 1997). We also note here that observational studies indicate that, for non-mass-transfer binaries containing low-mass stars, the distribution of values of q may peak toward small values (e.g., q^{-1} [Trimble 1990], or a Gaussian centered on $q = 0.23$ [Duquennoy & Mayor 1991]). If such distributions apply to a significant number of binary lenses, then the fraction of gently perturbed light curves becomes larger. The reason for this is that the linear dimensions of typical caustic structures become smaller as q decreases.

This brief discussion makes it clear that it is important for the observing teams to have at their disposal a method of reliably identifying and interpreting *all* binary-lens light curves.

1.2. Plan of the Paper

Section 2 describes our classification scheme and its application. Given a light curve, our goal is to find any and all binary-lens light curves that provide acceptable fits to it. Smooth light curves are considered in §2.3 and extremely perturbed light curves, including those with caustic crossings, are considered in §2.4.

We find that the light curves are highly degenerate, in that many distinct physical lensing events can create essentially identical light curves. An important feature of our method is that it identifies all physical solutions that are equivalent up to any chosen level as a function of photometric precision. In §3 we address the general question of distinguishing between true microlensing light curves and others that may have similar characteristics. We find that it is possible to use our method to eliminate many “pretenders” as well as to identify the possible physical parameters of true binary-lens events. In §4 we discuss the implications and possible extensions of this work.

2. Classification Scheme

2.1. Physical Characterization of the Lensing Events

The physical event that gives rise to a light curve can be characterized by the following quantities: (1) the binary’s total mass, $M = m_1 + m_2$ (with $m_1 > m_2$); (2) the ratio of the components’ mass, $q = m_2/m_1$; (3) a_{orb} , the projected separation on the lens plane between m_1 and m_2 ; (4) the distance of closest approach, b , between the track of the source and the binary’s center of mass; and (5) the angle of approach, θ , as measured with respect to the binary axis (with the direction from m_1 to m_2 defining $\theta = 0$). We will normalize to $M = 1$, thus allowing us to specify any lensing event by the set of physical parameters $p = \{q, a_{\text{orb}}, b, \theta\}$, where the first two elements describe properties directly related to the binary and its orientation in space, and the last two describe characteristics of the lensing event. All distances are measured in terms of R_E , the Einstein radius associated with the total mass, M . In principle, the full orbital solution of the binary serving as the lens could come into play if, for example, the time duration of the event is a considerable fraction of the orbital period. We return to this point in §4.

2.2. Classification of the Light Curves

Our thesis is that, if a microlensing model fits the data, then there is a high probability that the light curve is actually due to microlensing. The viability of this conjecture is discussed in §3. Use of the conjecture implies, however, that the primary challenge is to identify all microlensing light curves that fit the data. A simple method to do this is introduced in §2.3. This straightforward approach is all that is needed to identify all light curves that fit any smooth function. The application of an extended approach to extremely perturbed light curves, including those exhibiting singularities, is described in §2.4.

2.2.1. A Note on Degeneracy

In general, genuine binary microlensing light curves can be fit by many different lens models; as for the point-mass lens, there is a high degree of degeneracy. Also as in the case of the point lens, the degeneracy is due to symmetry. The symmetry is of two types: first is

symmetry inherent in the pattern of isomagnification contours. For example, several angles of approach may be equivalent slices through the geometry of a given lens. Secondly, there are slices through the lens plane of different lenses that (because of scaling, for example) are essentially equivalent. Because of this degeneracy, it is not adequate to find one or even a few possible binary models. Instead, we would like to find all binary lens models; this not only ensures that the correct model is among the ones we know about, it also allows the use of probability methods to study properties of the lens population.

2.2.2. Classification

The set of physical parameters, $\{p_i\}$, describes an event, i , that gave rise to a binary-lens light curve. The light curve itself can be characterized by a separate set of parameters, which describe its shape, independent of the physical event that produced it. For the sake of clarity, we will refer to this second set of parameters as the light curve parameters. For example, the coefficients of a polynomial expansion provide a complete set of light curve parameters for smooth light curves.

The basic idea behind our method is to characterize an observed light curve by a set of light curve parameters and to identify all binary lens light curves characterized, within the limits of observational uncertainty, by the same parameters.

2.3. Expansion of A Smooth Light Curve

Our approach is mathematical, but can be applied to real light curves. The basic idea is to treat each light curve as a mathematical function $A(t)$ which can be expanded in terms of a complete set of orthonormal functions

$$A(t) = \sum_{n=0}^{\infty} a_n T_n(t) , \quad (1a)$$

where,

$$\int_{-\infty}^{\infty} T_n(t) T_j(t) w(t) dt = \delta_{nj} , \quad (1b)$$

$w(t)$ is a weight function whose form is specific to the set of base functions $T_n(t)$, and

$$a_n = \int_{-\infty}^{\infty} A(t) T_n(t) w(t) dt. \quad (1c)$$

In this way, every light curve is completely specified by the values of the set of coefficients $\{a_n\}$. We may thus view the light curves as residing in the space of the coefficients.

This mathematical expansion not only provides a systematic way to characterize each light curve, but also to quantify the degree of similarity between different light curves. If two light curves are similar (i.e., of similar shape and encompassing nearly equal areas) then the coefficients of their expansions will be close in a way that can be quantified. Indeed, the condition

$$\int_{-\infty}^{\infty} [A(t) - A'(t)]^2 w(t) dt < \epsilon \quad (2a)$$

is equivalent to

$$D^2 = \sum_{n=0}^{\infty} [a_n - a'_n]^2 < \epsilon. \quad (2b)$$

Thus, distances in the space of the light curves can be measured with a Euclidean metric. (Bolatto & Falco, e.g., used an observation-based approach parallel to this.)

While any complete, orthonormal set of functions can be used to expand the light curves, some choices have advantages over others. We have chosen to use the Tchebyshev polynomials, $T_n(x)$.¹ The special charm of the Tchebyshev polynomials for the expansion of smooth light curves is that the convergence is rapid, and, in addition, for smooth light curves the expansion can be truncated in such a way as to mimic photometric errors of a predetermined size, consistent with the observations of any given light curve. This is as follows.

Suppose that we have expanded a light curve, which has been frequently sampled, to order N . It is important to know how well the light curve can be approximated if we truncate the expansion at lower order, m . Indeed, since the $T_k(x)$'s are all bounded between plus and minus 1, the discrepancy can be no larger than the sum of the absolute value of the neglected a_k 's ($k=m+1, \dots, N$). If the a_k 's are rapidly decreasing (which is the case for smooth light curves, see also Fig. 2), then the error is dominated by $a_{m+1}T_{m+1}(x)$, an oscillatory function with $m+2$ equal extrema distributed smoothly over the interval $[-1,1]$. Thus, the error is spread uniformly over the whole interval. We can now use this formalism to mimic the observational uncertainties. Given the size of photometric errors

¹The Tchebyshev polynomials can be expressed as $T_n(x) = \cos(n \arccos(x))$. They are defined and orthogonal on the interval $[-1,1]$, over a weight $w(x) = (1 - x^2)^{-1/2}$. We have $T_0(x) = 1$, $T_1(x) = x$; the recursion relation $[T_{n+1}(x) = 2xT_n(x) - T_{n-1}(x)]$ can be used to derive the functional form of T_n for $n > 1$. T_n has n zeros and $n+1$ extrema on the interval $[-1, 1]$.

(say $\delta = 1\%$), we can terminate the expansion of the light curve at the order at which $a_{m+1} \sim \delta$ (where a_0 has been normalized to unity). A similar cut-off should also be applied to those numerically-generated light curves to which the observed curve is being compared, so that they can, in effect, be sampled with a photometric precision comparable to that achieved for the data.

Given an observed light curve, we compute a Tchebyshev expansion as follows. First, the time interval over which the light curve is sampled must be mapped onto the interval $[-1,1]$. This can be done by studying the “wings” of the light curve, as the magnification just begins to rise above (and then to fall below) unity; we have chosen the cut-off magnification to be 1.06, corresponding to a distance of $2R_E$ from a point mass lens. The interval $[t_{up}, t_{down}]$ (from the baseline just before the event begins to the baseline just after the event ends) is mapped onto the interval $[-1,1]$. Then, we compute the expansion coefficients, a_n . Instead of using the expression in (1a), we do a somewhat different expansion:

$$A(t) = \sum_{n=0}^m a_n T_n(t) - \frac{1}{2} a_0. \quad (3)$$

This alternative expansion has the useful feature that it is guaranteed to exactly agree with the observed light curve at m points, the positions of the m zeros of T_m (see, e.g., Press *et al.* 1992).

2.3.1. Equivalent Light Curves

The $\{a_n\}$ characterize the light curve, to whatever level of precision we have chosen. Our ultimate goal is to use this characterization to identify all binary lens light curves which, to the same level of precision, are equivalent to the original one. If the light curve we started with, drawn from the data, is indeed due to lensing by a binary, then we would like to find all sets of the physical parameters $p_i = \{q_i, a_{\text{orb},i}, b_i, \theta_i\}$ that could have given rise to it. We would also like to know, with some level of confidence, if the observed light curve is not due to binary lensing.

Therefore, given the light curve and its expansion, we proceed to identify all binary lens light curves that are essentially indistinguishable from it where our criterion for indistinguishability is set by Eqn.(2b), with ϵ determined by the photometric error. For a given level of photometric uncertainty, δ , ϵ should be chosen to be roughly equal to 2δ , since $\delta \times \{\int_{-1}^1 dt\} \sim \epsilon$.

The simplest version of our method consists of looking for light curves that provide good fits to the original by randomly generating a large number of lensing events, p_i ,

finding the light curve expansion of each, and computing the distance, in the space of the coefficients, between the light curve and the original. Those sets of physical parameters with light curves which lie close to the light curve of the original in the space of the coefficients, are candidates for the physical lensing event that gave rise to the original light curve.

2.3.2. Improved Sampling

A completely random sampling is numerically inefficient; it is preferable to first identify all regions of the parameter space in which there is some possibility of finding a match. We can do this by maintaining a “library” of event characteristics. The library relates the physical parameters describing an event to the light curve parameters that characterize the resulting light curve. Each line of the library is specified by the values $\{q_i, a_{\text{orb},i}, b_i, \theta_i\}$ used to generate a light curve; the other entries include the locations and values of the magnification at extrema and inflection points. We begin by searching through the library for those light curves whose gross features are consistent with those of the observed light curve. Specifically, we identify physical events (i.e., sets of physical parameters) that generate light curves with positions of extrema and inflection points, and magnifications at these points, within roughly 10% of those of the observed light curve. The physical parameters of each such library member represent an event whose gross morphological properties are similar to those of the observed light curve. These points in the parameter space therefore provide a starting point for a finer sampling of a small region of the parameter space. It is this finer sampling which yields the matching light curves. Figure 2 shows three examples; the sampling is described in the caption. The degree to which the parameter space sampling can influence the discovery of degenerate solutions, and to which improved photometric precision can help to break degeneracies, is demonstrated in Figures 2 and 3, respectively.

How many events need to be included in the library, if we are to be certain that we have carried out a smooth sampling of the parameter space? If the morphology of a light curve (i.e., positions of extrema, for example) changed dramatically when the physical parameters specifying the event changed but little, a comprehensive library would need to be large. Fortunately, the morphological features change in a way that is gradual and consistent as the physical parameters are changed (see Fig.4), so that a library with $\mathcal{O}(10^5)$ events appears to be adequate.

2.4. Singular or Sharply Peaked Light Curves

Consider a case in which the track of the source does not pass close to the caustic structure associated with the binary lens. The light curve will be smooth and, generally, only few terms are needed in order for the Tcheychev expansion to provide a good approximation to it. (For example, a_{10} , the sixth even coefficient in the expansion of the first light curve in Figure 2 is only 1% of a_0 ; the odd coefficients are all below the 1% level.) If we allow the track of the source to come closer to the caustic structure we will obtain light curves that become ever more sharply peaked. These light curves can formally be expanded, but an expansion to reasonable order will not provide a good approximation to the light curve. (See the middle set of panels of Figure 2.) Nevertheless, the expansion coefficients, augmented by the the values of the gross morphological parameters, can indeed be used to characterize even the most extremely perturbed light curve.

Just as in the case of light curves observed to be smooth, we search through the library to identify all sets of physical parameters p_i 's giving rise to light curves with similar gross features. If the gross features match to within a chosen level of precision ($\sim 10\%$) we then compute, in the region around each such p_i , light curves for large numbers of randomly generated sets of physical parameters. When condition (2b) is satisfied, we are guaranteed that the two light curves are equivalent, to the level of precision we have chosen.

It is interesting to note that neither light curve will match the expansion, which has inflection points and extrema not shared by the light curves. But the two light curves and the expansion agree at the m zeros of $T_m(t)$, and, in addition, the two light curves agree at all extrema and inflection points. The two light curves are therefore equivalent. In general, we find that the shape of even extreme light curves is determined by the value of the magnification at a relatively small number of points.

3. False Positives: Eliminating the Pretenders

Given the tremendous diversity of binary-microlensing light curves, it has been conjectured that essentially *any* light curve can be well-fit by a binary-lens model. If this conjecture is true, then it poses a serious problem for the analysis of data from the monitoring programs. The true rate of lensing would never be known, since virtually any form of stellar variability that is neither continuous nor repeating could be interpreted as a microlensing event. Fortunately, the validity of this conjecture can be constrained in a

quantifiable way. First we consider individual light curves, and then ensembles of light curves.

The morphology of a light curve is determined by the topology of the isomagnification contours. This is determined by the physics of the microlensing process. Although many variations are associated with the many possible sets of values of the physical parameters of the lensing events, it is not true that a binary-lens light curve can take on any arbitrary functional form. There are a few obvious constraints. For example, although light curves can be singular (or, taking finite-source-size effects into account, nearly singular, exhibiting sharp rises and declines), the number of such singularities is constrained by the fact that each represents a crossing through a closed caustic curve. Thus, there are always an even number of caustic crossings. Even when the track of the light curve grazes the caustic structure, so that the time between the passage into and out of the closed curve is small—perhaps too small to resolve—the magnification before and after the double passage must be consistent with a grazing incidence, and this itself provides constraints. Furthermore, the magnification within the caustic structure has a well-defined minimum (Witt & Mao 1995). Similarly, the positioning and magnification of smooth peaks cannot be arbitrarily arranged. Even a function with a single peak can be distinctive enough that a binary lens model simply cannot fit. We have carried out a test to determine whether a specific blended point-lens light curve could be mis-identified as a binary lens light curve. First we generated a point-mass lens light curve; out of 10^5 randomly generated binary-lensing events, we found that 753 were equivalent to it if the uncertainty in the photometry were at the 2% level. However, under the same conditions, no equivalent binary-lensing event was found for the blended version of this light curve. (We assumed that the lensed source contributed 10% of the baseline flux.) This test provides a simple, quantifiable counterexample to the conjecture that any light curve can be fit by some binary lens model.

As in the example cited above, the failure to find good matches is operational, subject to the conditions under which the search has been conducted, which must always be explicitly stated. With this caveat, we note that the mathematical formalism we have used provides a concrete and well-defined way to test the conjecture that any specific function can be well-fit by a binary-lens model. The level at which a search rules out a binary fit can be specified and, if a binary lens fit does work, the degeneracy of the physical solutions can also be fully worked out.

Another way to see that binary lens light curves do have distinctive characteristics that cannot be mimicked by arbitrary functional forms, is to examine the distribution of binary lens light curves in the parameter space defined by the coefficients $\{a_n\}$. The conjecture

that any light curve can be fit by a binary lens model is equivalent to the conjecture that the coefficient space is everywhere dense in points corresponding to binary lens light curves. In Figure 5 we study the pattern of points in the coefficient space associated with smooth double-peak light curves. It is obvious that there is a pattern, and not a uniform distribution. The pattern is so distinctive that it is possible to clearly detect the presence of a cloud of points that is somewhat deviant from it. This cloud of points actually defines a distinct distribution: double-peak light curves in which the magnification dips below 1.34 between peaks, so that one is in essence watching two separate lensing events (Di Stefano & Mao 1996). Thus, the figure demonstrates that the coefficient space distribution of points associated with binary lens light curves contains useful information. In addition, Figure 5 shows that blending serves to shift the distribution of light curves in the parameter space. This is another demonstration of the link between the physical characteristics of a light curve, and the position of the corresponding point in the space of the coefficients.

4. Applications and Extensions

4.1. Applications

What are the prospects that binary lens events that might otherwise have been missed, will be successfully identified via our method? It is already known that the fit between the data and lens model for some light curves identified as being due to lensing by a single mass, can be marginally improved by using a binary lens model (see, e.g., Dominik & Hirshfeld 1996). In such cases, it is questionable whether the introduction of new parameters to effect a marginal improvement should be viewed as strongly supporting the hypothesis that the lens was actually a binary. The key to a successful model is that the fit to the data should be convincingly better than to a point-lens model. The light curve must therefore be distinctive (as the OGLE 7 event was, for example, and as many smooth binary lens light curves are), or the photometry and sampling must be better than is typical for the monitoring teams. Since we cannot easily order up distinctive events, we can act to improve the situation only through improved monitoring. Fortunately, the benefits of more frequent sampling of ongoing events and real-time analysis are now being realized through the combined efforts of the monitoring teams, who announce their discovery of events as soon as possible, and independent groups of observers who have designed observational programs to provide frequent coverage of ongoing events (see, e.g., Albrow *et al.* 1996; Alcock *et al.* 1996). In principle, the follow-up teams, who have access to telescopes positioned around the Southern hemisphere, can monitor events hourly, from the time of first notification

until the event is finished. Furthermore, because the follow-up teams are most interested in deviant light curves, particularly if there is a chance that they are due to lensing by a planetary system, their photometric measurements tend to be sensitive, with uncertainties at the 1 – 2% level. During their 1996 observing season, the PLANET collaboration followed the progress of 2 events in the LMC and 31 in the direction of the Galactic Bulge; in 1995 they studied 41 Bulge events (www.astro.rug.nl/~planet). The ascendancy of these follow-up programs and proposals to implement even more sophisticated monitoring programs, improve our chances of detecting deviant light curves. The next step in our research program is therefore to work with several of the teams to fashion an application of the method which carefully considers and meshes the issues of observational and coefficient space sampling.

4.2. Other Perturbations

The method we have developed can be applied to light curves that differ from the standard because of any astronomical effect, e.g., blending, parallax, finite source size. The more complicated the effect (such as finite source size) or the more effects we want to consider, the larger the number of relevant physical parameters becomes. Let's therefore augment the set of physical parameters, $\{p_i\}$, by adding an additional set of parameters, $\{P_i\}$ to describe all of the other physical effects that may be relevant. Since the method outlined in §2 is completely general, an obvious way to proceed would be to simply use a parallel approach, including the full set of parameters, $\{p_i, P_i\}$, instead of just $\{p_i\}$. This brute force approach would generally not be computationally efficient, however. The library of events for the preliminary comparison would be large, and the regions we would need to subsequently sample in the parameter space would be of high dimension.

Especially when the additional effects can be easily expressed analytically, as they can, e.g., for blending and for velocity effects (including parallax and the orbital motion of the lens if it is a binary) there is a more efficient way to proceed. Because the influence of these additional effects on the light curve can be expressed analytically, we could, if we knew the values of the $\{P_i\}$, effectively eliminate them, to derive a residual light curve having either the form of a point-lens light curve or of a multiple system, such as a binary lens. Of course we don't know the values of the $\{P_i\}$ *a priori*. But the form of the observed light curve generally allows us to set some limits on the range of values of each parameter that might be relevant. Thus for each of a randomly sampled set of parameters, $\{P_i\}$, within the appropriate range, we can derive a “residual” light curve and then apply the method outlined in §2.

4.3. Conclusion

The principle features of an approach to systematically study light curves perturbed because of lens binarity or any other astronomical effect have been outlined. The application of the approach has been demonstrated.

One important feature of this work is that it provides a unified approach for the identification and study of all binary lens light curves, and indeed, all light curves perturbed from the standard point-mass lens form. Perhaps equally important, is that it provides a systematic way to quantify the degeneracy of the physical situations which could possibly have given rise to any particular observed light curve. This is important because, unless the extent of the degeneracy is fully understood, it is not possible to use an ensemble of light curves to place meaningful constraints on the true distribution of lens parameters. We have found that, as may well be expected, the level of degeneracy for binary lens light curves is highest for light curves with the fewest distinctive features, i.e., those most like the standard point-mass lens light curves. This result emphasizes the challenge of distinguishing point-lens events from binary lens events, and thereby also serves to reinforce the need for the type of frequent, sensitive follow-up which has been tested during the past two years (see, e.g., Albrow *et al.* 1996; Alcock *et al.* 1996). We note, in addition, that a large fraction of binary lens light curves are neither close to the point-lens form, nor as extremely perturbed as the binary lens light curves discovered in the data so far. These are the light curves whose apparent absence in the data set is puzzling. It remains to be determined if the lack of such events may be indicative of problems with the detection efficiency, perhaps related to the use of a set of detection criteria that is too narrow.

The challenge for the future is to use the principles outlined here to study real data. There are almost certainly light curves in the present data set which could tell us more about the events that gave rise to them through application of a method such as the one presented here. There will certainly be light curves observed by the follow-up teams for which this will be the case. Applying these principles to the data will guide us to more refined and efficient approaches. But, most importantly, work along these lines will help us to learn more about the population of stellar and dark lenses in the Local Group.

Acknowledgments

This work was supported in part by NSF GER-9450087. We also thank the anonymous referee for comments that helped us to clarify the presentation.

REFERENCES

Alard, C., Mao, S., & Guibert, J. 1995, A&A, 300L, 17.

Albrow, M., et al. 1996, astro-ph/9610128.

Alcock, C., et al. 1996, ApJ, 1996, 463L, 67.

Bennett, D., et al. 1996, NuclPhysB, in press (astro-ph/960612).

Bolatto, A. D., & Falco, E. E. 1994, ApJ, 436, 112

Buchalter, A., Kamionkowski, M., & Rich, R.M. 1996, ApJ, 469, 676.

Di Stefano, R., 1997, in preparation.

Di Stefano, R., & Mao, S., 1996, ApJ, 457, 93.

Di Stefano, R., & Esin, A. 1995, ApJ, 448L, 1.

Dominik, M., & Hirshfeld, A.C. 1996, A&A, 313, 841.

Duquennoy, A., & Mayor, M. 1991, A&A, 248, 485.

Griest, K., & Hu, W. 1992, ApJ, 397, 362

Kamionkowski, M. 1995, ApJ, 442L, 9.

Mao, S., & Paczyński, B. 1991, ApJ, 374, L37

Mao, S., & Di Stefano 1995, ApJ, 440, 22

Paczyński, B. 1986, ApJ, 304, 1

Press, W.H., Teukolsky, S.A., Vetterling, W.T., & Flannery, B.P. 1992, *Numerical Recipes*, Cambridge University Press.

Trimble, V. 1990, MNRAS, 242, 79

Witt, H.J. 1995, ApJ, 449, 42

Witt, H.J., & Mao, S. 1994, ApJ, 430, 505

Witt, H.J., & Mao, S. 1995, ApJ, 447, L105

Udalski, A., Szymański, M., Mao, S., Di Stefano, R. I., Kałużny, J., Kubiak, M., Mateo, M., Krzeminski, W. 1994, ApJ, 436, L103

Figure 1.– These 15 light curves have been randomly generated, with all of the physical variables (§2.1) chosen from uniform probability distributions. The mass ratio was chosen to have values ranging from 0 to 1, the orbital separation varied between 0 and $1.8R_E$, the inclination of the source track relative to the binary axis varied from 0 to 2π , and the distance of closest approach varied between 0 and $1R_E$. The only restriction placed on the light curves shown here, is that the integrated area under the light curve must differ by more than 1% from the area under the point-mass lens light curve most similar to the one shown. By the point-lens light curve most similar to the one shown, we mean the point-lens light curve that matches exactly in the wings (i.e., at $x = +1$ and $x = -1$) and that bounds the same area from above.

Figure 2.– Three binary lens light curves (left set of panels) were generated by three physical events, specified by the values $\{q_0, a_{\text{orb},0}, b_0, \theta_0\}$. A Monte Carlo approach was used to sample the entire parameter space of physical variables to find other events that generate nearly identical light curves. Each of these new events served as a seed for further sampling of a small region. The middle set of panels show all the physical binaries (a_{orb} vs $\log(q)$) we found that can, with appropriate choices of b and θ , give rise to light curves whose integrated deviation from the one shown is smaller than 2%. Note that the level of degeneracy generally declines as the number of distinctive light curve features (extrema and inflection points) increases. Other points of interest: (1) good uniform sampling is needed in the first step of the search to prevent the clumpiness produced by our seeding in the top middle panel. (2) Binary separations of $2R_E$ still yield events with clear evidence of lens binarity. Finally, the set of panels on the right show the first 50 Tchebyshev coefficients for the corresponding light curve in the left-most panel. The coefficients are expressed in units of a_0 . Note that the smoother the light curve, the faster the convergence.

Figure 3.– The integrated deviation between the top light curve in Figure 1 and the “nearest” point-mass light curve is $\sim 1.5\%$. This is shown in the top panel, with the point-by-point difference between the light curves plotted in the middle panel. The bottom panel illustrates that, even if the photometry were good enough to distinguish between the binary lens and point-mass light curves shown in the top panel, the binary lens light curve would still be degenerate. Points in the bottom panel are associated with light curves that differ from the original by less than 1%.

Figure 4.– Variation in the amplitude of a light curve as the parameters are varied. In the left panel the parameters $a_{\text{orb}}, \theta, q$ are kept fixed while the impact parameter b changes by 0.1 from light curve to light curve. In the set of panels on the right, the parameters a_{orb}, q, b are kept fixed while θ changes by $\pi/6$ from light curve to light curve.

Figure 5.– Points in the coefficient space of all smooth double-peak binary lens light

curves found in a sampling of $\sim 200,000$ events with $b < 1R_E$. a_0 has been normalized to unity. The top left panel is a_4 vs a_2 ; in the second row are a_6 vs a_2 , and a_6 vs a_4 , respectively; the ordering of axes continues in this way in rows 3 and 4. Note that, not only is the general pattern of points striking, but also that deviations from it can be specifically linked to light curve features. The diffuse cluster of points near the origin in each panel corresponds to smooth double-peak light curves that would likely be perceived as repeating events. The main pattern of points traces the placement of continuous smooth perturbations with $A > 1.34$ throughout. This is demonstrated in the top two panels on the right. The panel just below these shows that, even in a single plot, the effects of blending can be distinguished. The dots are the same as in the top left panel; the circles are blended, smooth, 2-peak binary lens events. Peak placement and relative peak and valley magnifications are the same as for the other binary lens light curves, thus representing a particularly mild perturbation of standard binary lens light curves; it is therefore interesting that the difference can be distinguished on this scale.

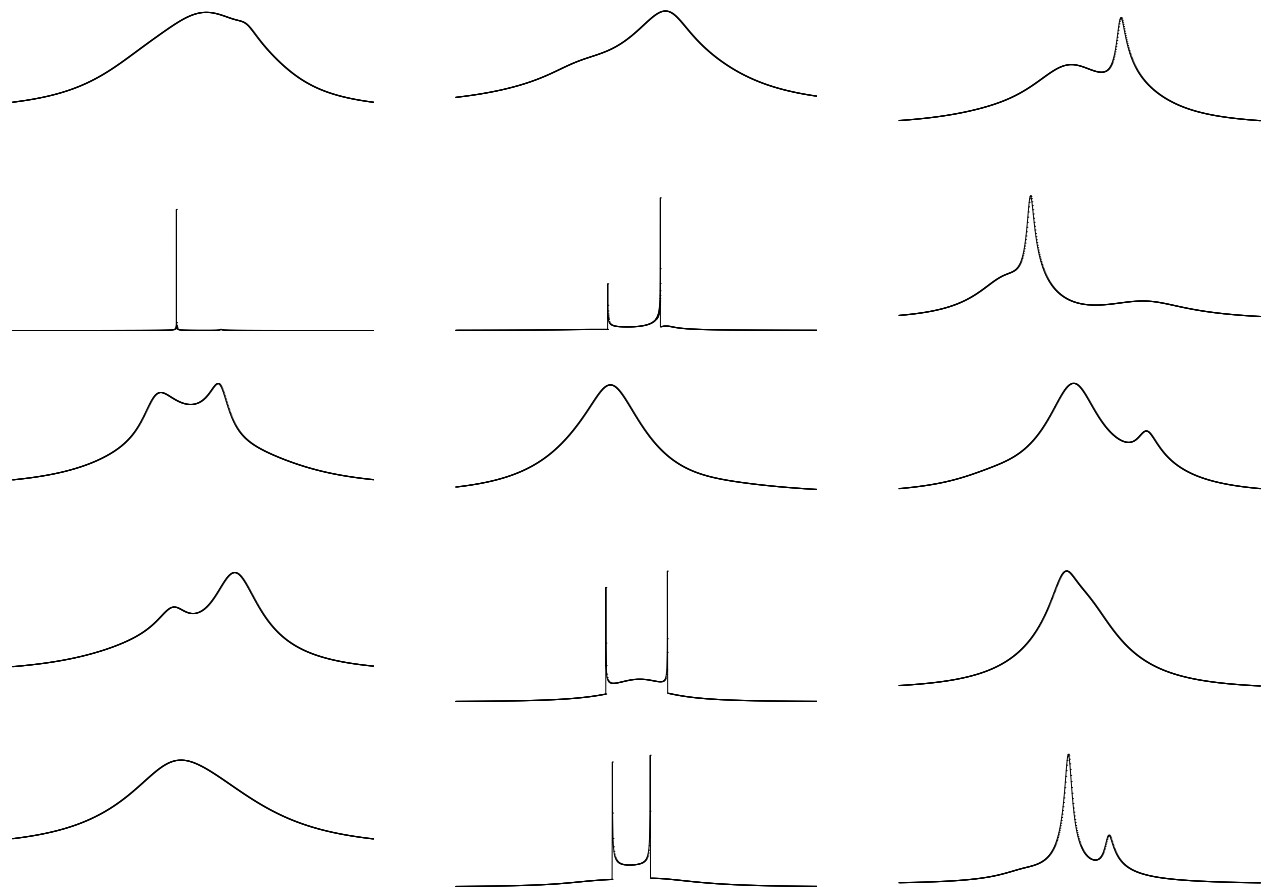


Figure 1

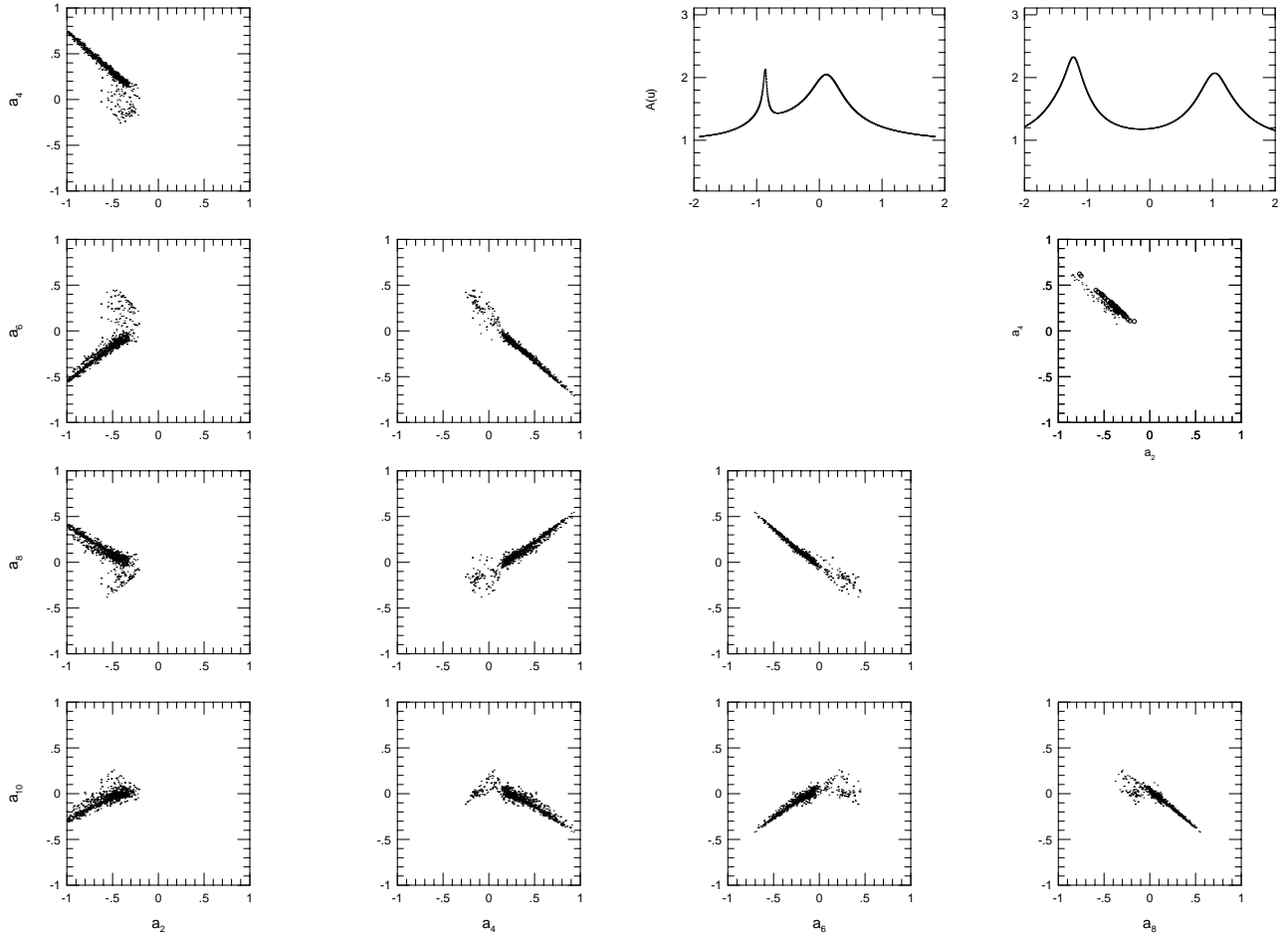


Figure 5